

qNMR quantification and *in silico* analysis of isobrucein B and neosergeolide from *Picrolemma sprucei* as potential inhibitors of SARS-CoV-2 protease (3CLpro) and RNA-dependent RNA polymerase (RdRp) and pharmacokinetic and toxicological properties

Quantificação por qRMN e análise *in silico* de isobruceína B e neosergeolida de *Picrolemma sprucei* como potenciais inibidores de protease SARS-CoV-2 (3CLpro) e RNA polimerase dependente de RNA (RdRp) e propriedades farmacocinéticas e toxicológicas

Cuantificación por qNMR y análisis *in silico* de isobruceína B y neosergeolida de *Picrolemma sprucei* como inhibidores potenciales de la proteasa del SARS-CoV-2 (3CLpro) y la ARN polimerasa dependiente de ARN (RdRp) y propiedades farmacocinéticas y toxicológicas

Received: 11/12/2021 | Reviewed: 11/20/2021 | Accept: 11/25/2021 | Published: 12/07/2021

Marcos Túlio da Silva

ORCID: <https://orcid.org/0000-0002-7653-4944>
Universidade Federal do Amazonas, Brasil
E-mail: marcostulio39@gmail.com

Matheus Gabriel de Oliveira

ORCID: <https://orcid.org/0000-0003-0692-9729>
Universidade Federal de Goiás, Goiânia, Brasil
E-mail: matheusgabriel06@hotmail.com

José Realino de Paula

ORCID: <https://orcid.org/0000-0002-4424-7692>
Universidade Federal de Goiás, Brasil
E-mail: pjrpaula@gmail.com

Vinicius Barreto da Silva

ORCID: <https://orcid.org/0000-0002-5066-7431>
Pontifícia Universidade Católica de Goiás, Brasil
E-mail: viniciusbarreto.farmacia@gmail.com

Kidney de Oliveira Gomes Neves

ORCID: <https://orcid.org/0000-0001-5238-4243>
Universidade Federal do Amazonas, Brasil
E-mail: kidneydeoliveira@gmail.com

Marcos Batista Machado

ORCID: <https://orcid.org/0000-0002-8791-4803>
Universidade Federal do Amazonas, Brasil
E-mail: marcosmachado@ufam.edu.br

Rita de Cássia Saraiva Nunomura

ORCID: <https://orcid.org/0000-0002-1119-7238>
Universidade Federal do Amazonas, Brasil
E-mail: ritasnunomura@gmail.com

Abstract

Objective: To quantify the quassinoids of *P. sprucei*, a medicinal plant that is native to the Amazon region, using qNMR and investigate the inhibitory potential of isobrucein B and neosergeolide on the 3CLpro and RdRp targets of SARS-CoV-2 through *in silico* approaches. **Methods:** the quantification was performed in a fraction (F2-F3) enriched with the quassinoids isobrucein B and neosergeolide using the PULCON method. *In silico* assays were performed using molecular docking to assess interactions and binding affinity between neosergeolide and isobrucein B ligands with SARS-CoV-2 3CLpro and RdRp targets, and online servers were used to estimate pharmacokinetic and toxicity. **Results:** It was possible to determine the quantity of the two quassinoids isobrucein B and neosergeolide in the F2-F3 fraction (769.6 mg), which were present in significant amounts in the PsMeOH extract (5.46%). The results of the docking analysis, based on the crystallized structures of RdRp and 3CLpro, indicated that isobrucein B and neosergeolide are potential inhibitors of the two proteins evaluated, as well as showing the importance of hydrogen bonding and pi (π) interactions for the active sites foreseen for each target. **Conclusion:** The results suggest that *P. sprucei* quassinoids may

interact with 3CLpro and RdRp targets. *In vitro* and *in vivo* experiments are needed to confirm the results of molecular docking and investigate the risks of using *P. sprucei* as a medicinal plant against COVID-19.

Keywords: Quassinoids; Caferana; Molecular Docking; qNMR; SARS-CoV-2.

Resumo

Objetivo: Quantificar os quassinóides de *P. sprucei*, uma planta medicinal nativa da região amazônica, usando qRMN e investigar, o potencial inibitório da isobruceína B e neosergeolida nos alvos 3CLpro e RdRp da SARS-CoV-2 por meio de abordagens *in silico*. **Métodos:** a quantificação foi realizada em uma fração (F2-F3) enriquecida com os quassinóides isobruceína B e neosergeolida pelo método PULCON. Os ensaios *in silico* foram realizados por meio de docking molecular para avaliar a interações e afinidade de ligação entre os ligantes neosergeolida e isobruceína B com os alvos 3CLpro e RdRp da SARS-CoV-2 e servidores online foram utilizados para estimar os parâmetros farmacocinéticos e de toxicidade. **Resultados:** foi possível determinar a quantidade em mg dos dois quassinóides isobruceína B e neosergeolida na fração F2-F3 (769.6 mg), presentes em quantidades significativas no extrato PsMeOH (5,46%). Os resultados da análise de docking, com base nas estruturas cristalizadas de RdRp e 3CLpro, indicou isobruceína B e neosergeolida indicou que isobruceína B e neosergeolida são inibidores potenciais das duas proteínas avaliadas, bem como mostrou a importância da ligação de hidrogênio e interações pi (π) para os sítios ativos previstos para cada alvo. **Conclusão:** Os resultados sugerem que os quassinóides de *P. sprucei* podem interagir com os alvos 3CLpro e RdRp. Experimentos *in vitro* e *in vivo* são necessários para confirmar os resultados de docking molecular e investigar os riscos de *P. sprucei* como planta medicinal contra a COVID-19.

Palavras-chave: Quassinoides; Caferana; Docking molecular; qRMN; SARS-CoV-2.

Resumen

Objetivo: Cuantificar los cuassinoides de *P. sprucei*, una planta medicinal nativa de la región Amazónica, mediante qNMR e investigar a través de enfoques *in silico*, el potencial inhibitorio de isobruceína B y neosergeolida sobre objetivos 3CLpro y RdRp del SARS-CoV-2. **Métodos:** la cuantificación se realizó en una fracción (F2-F3) enriquecida con los cuassinoides isobruceína B y neosergeolida, utilizando qRMN por el método PULCON. Se realizaron ensayos *in silico* utilizando acoplamiento molecular para evaluar las interacciones y la afinidad de unión entre los ligantes de neosergeolida e isobruceína B con objetivos de SARS-CoV-2 3CLpro y RdRp, además se utilizaron servidores en línea para estimar la farmacocinética y la toxicidad. **Resultados:** se pudo determinar la cantidad en mg de los dos cuassinoides isobruceína B y neosergeolida en la fracción F2-F3 (769,6 mg), presentes en cantidades significativas en el extracto de PsMeOH (5,46%). Los resultados del análisis de acoplamiento molecular, basados en las estructuras cristalizadas de RdRp y 3CLpro, indicaron que isobruceína B y neosergeolida son inhibidores potenciales de las dos proteínas evaluadas, además de mostrar la importancia de los enlaces de hidrógeno y las interacciones pi (π) para los sitios activos previstos para cada objetivo. **Conclusión:** Los resultados sugieren que los cuassinoides de *P. sprucei* pueden interactuar con los objetivos 3CLpro y RdRp. Se necesitan más investigaciones y experimentos *in vitro* e *in vivo* para confirmar los resultados del acoplamiento molecular e investigar los riesgos de *P. sprucei* como planta medicinal contra COVID-19.

Palabras clave: Cuassinoides; Caferana; qRMN; Acoplamiento molecular; SARS-CoV-2.

1. Introduction

The SARS-CoV-2 coronavirus pandemic emerged in Wuhan, China, with the first infections being reported in December 2019 (COVID-19). Due to its rapid spread, by June 2021, more than 178 million cases of the disease had been registered worldwide, and deaths already surpass three million people (World Health Organization [WHO], 2021). Representing an unprecedented challenge, extensive research into developing new antiviral drugs for COVID-19 has identified potential targets that play an important role in blocking viral infection (Ghahremanpour et al., 2020).

Chinese research groups have sequenced the SARS-CoV-2 genome and its non-structural proteins (NSP), including the spike protein, 3-chymotrypsin-like cysteine protease (3CLpro), also called the major protease (Mpro), papain-like protease (PLpro), and RNA-dependent RNA polymerase (RdRp) (Zhu et al., 2019; Morse et al., 2020). The protein's role is to bind the virus to the human receptor – a metallopeptidase called angiotensin-2 converting enzyme (ACE2), while 3CLpro and PLpro provide components to pack new virions of large translated viral polyproteins into the host ribosome, and finally, RdRp replicates the SARS-CoV-2 RNA genome (Morse et al., 2020).

The 3CLpro and RdRp targets have great importance in the viral replication of SARS-CoV-2 and stand out as essential targets in computational strategies such as molecular docking (Qamar et al., 2020; Wu et al., 2020; Das et al., 2020; Yu et al., 2020). Molecular docking is currently being used as a powerful tool in addition to being rational and low-cost for screening new

antiviral agents against COVID-19 and allows us to understand how these NSPs are important targets of SARS-Cov-2 and how they will interact with ligands at the active site (Qamar et al., 2020; Wu et al., 2020; Das et al., 2020; Yu et al., 2020; Rahmatullah et al., 2020).

Regarding ligands, drugs used against other human diseases and natural products present in medicinal plants, such as flavonoids, and other bioactive compounds, such as quassinoids, have been used as candidates in virtual screening approaches. (Da Silva et al., 2020; Neves et al., 2021). In addition, the quassinoids are potential candidates in virtual screening approaches in the search for new agents against COVID-19 (Hasan et al., 2020; Qamar et al., 2020; Rahmatullah et al., 2020). Because they do not have easy access to medicines, a large part of the world population, including indigenous tribes, *quilombolas*, and riverine communities in the Amazon, resort to the use of medicinal plants, which in most cases are the only source of medicine for the treatment or cure of diseases (Le Cointe, 1947; Da Silva et al., 2020;)

Picrolemma sprucei Hook, from the Simaroubaceae family, is a native plant of the Amazon region that is popularly used as a medicinal plant, mainly for the treatment of malaria (Nunomura, 2006; Pohlit et al., 2009b; Ribeiro et al., 1999). It is popularly known in Brazil as “caferana” due to its similarity to *Coffea arabica* L. It can be found in street markets and through herbalists in the region and is marketed as an antimalarial and for the treatment of fevers, in the Adolpho Lisboa Municipal Market in Manaus (Cavalcante, 1983; Thomas 1990; Ribeiro et al., 1999; Ferreira, 2000; Saraiva et al., 2002).

The main constituents of *P. sprucei* are the quassinoids, which are only produced by species of this family. Quassinoids are biodegraded triterpenes and are highly oxygenated with a wide range of biological activities. Many quassinoids exhibit a wide range of biological activities *in vitro* and/or *in vivo*, including antiviral, antitumor, antimalarial, anti-inflammatory, antifeedant, insecticidal, amoebicidal, antiulcer, and herbicidal activities (Guo et al., 2005).

Previous research on the roots and stems of *P. sprucei* resulted in the isolation of the main quassinoids of this species, neosergeolide and isobrucein B (Moretti et al., 1982; Zukerman-schpecto & Castellano, 1994, Vieira et al., 2000, Saraiva, 2001, Amorim, 2009). Nunomura et al. (2006) demonstrated *in vitro* anthelmintic activity of isobrucein B and neosergeolide isolated from the chloroform fraction of *P. sprucei* against *Haemonchus contortus*. This nematode parasitizes the gastrointestinal system of sheep and other animals. Other *in vitro* studies report antitumor, antimalarial, anthelmintic, cytotoxic, insecticidal, and anti-leishmanial activities of neosergeolide and isobrucein B (Fukamiya, et. al., 2005; Almeida et al., 2007; Andrade-Neto, et al., 2007; Silva et al., 2009b).

Therefore, the present study quantified the quassinoids neosergeolide and isobrucein B of *P. sprucei* using NMR and the PULse Length-based CONcentration determination methodology (PULCON). qNMR has shown to be a less laborious and high precision alternative in the simultaneous quantification of organic compounds in a complex mixture (Oliveira et al., 2021). In addition, the study carried out the tracking analysis of these quassinoids using molecular docking, in order to test them as potential inhibitors of SARS-CoV- 23CLpro and RdRp and is the first work to report this analysis of neosergeolide and isobrucein B against COVID-19 target enzymes.

2. Methodology

2.1 Plant material

Plant material was collected in February 2018 in the Adolpho Ducke Forest Reserve in the city of Manaus, Brazil under geographic coordinates (02° 54' 48.2'' S, 59° 58' 49.2'' W) after obtaining authorization from the Biodiversity Authorization and Information System (SISBIO No. 46383). The botanical identification of the species as *Picrolemma sprucei* Hook.f. was carried out at the National Institute for Amazonian Research (INPA) by Mariana Rabello Mesquita. The exsiccate of the plant in the INPA herbarium is identified as 279918. Access to genetic heritage was registered (AE76F92) in the National System of Management of Genetic Heritage and Associated Traditional Knowledge (SisGen).

2.2 Plant material processing

The plant material was dried in a forced air circulation oven at 40 °C until completely dry. After drying, the material was separated into roots, stems, leaves, and fruits. Then, the part of the plant of interest in this work, the roots, was chopped into lengths of about 10 cm using pruning scissors and a hatchet, followed by fine grinding in a knife mill to obtain a fine powder (302.54 g).

2.3 Preparation of the plant extract

The *P. sprucei* root powder (302.54 g) was subjected to cold maceration (2 weeks) with hexane (1.0 L) with the aid of ultrasound to remove non-polar substances. This material was later extracted with methanol (1.0 L) via cold maceration. The methanol extract of *P. sprucei* root powder (PsMeOH) was obtained by exhaustive cold maceration (3 weeks). The PsMeOH was concentrated in a rotary evaporator (Fisatom® 801) at a temperature of 40 °C to remove all the solvent. After the complete drying of the PsMeOH extract, it was weighed to calculate the percentage of yield.

2.4 Phytochemical study

To obtain a fraction that was enriched in the constituents of interest (the quassinoids neosergeolide and isobrucein B), the dry crude methanolic extract was subjected to fractionation in classical column chromatography. The solvents used for the fractionation of the PsMeOH extract (10.43 g) were chloroform (CHCl₃) and methanol (MeOH) in a volume of 400 mL of the solvents in the following proportions: F1 (100% CHCl₃); F2 (97:3 CHCl₃/MeOH); F3 (95:5 CHCl₃/MeOH); F3 (90:10 CHCl₃/MeOH); F5 (80:20 CHCl₃/MeOH) and F6 (100% MeOH).

2.5 Analysis of fractions obtained from fractionation of PsMeOH extract by mass spectrometry (MS)

The spectrometry analyses of the fractions obtained from the fractionation of the PsMeOH extract were carried out at the Multidisciplinary Support Center – Analytical Center – CAM, located at the Federal University of Amazonas. The mass spectra were obtained by analysis in a triple-quadrupole spectrometer, (model TSQ Quantum Access Thermo scientific), equipped with an atmospheric pressure chemical ionization (APCI) chamber. For the analysis, 30 µL of each fraction was pipetted (filtered) and transferred to Eppendorf tubes and diluted in 1000 µL MeOH; this procedure was performed for the six samples. After this procedure, the samples were injected into the mass spectrometer with the APCI source in positive acquisition mode in a mass range (m/z) of 100-1000 Da. The obtained spectra were analyzed using *Xcalibur*® 2.0.7 software.

2.6 Identification and quantification of quassinoids via the PULCON method

The nuclear magnetic resonance (NMR) experiments were carried out at the Nuclear Magnetic Resonance Laboratory (NMRLab) of the Analytical Center (CA) of the Federal University of Amazonas (UFAM). One-dimensional (¹H, ¹³C, and DEPT135) and two-dimensional (COSY, HSQC, and HMBC) NMR spectra were obtained in a nuclear magnetic resonance spectrometer (Bruker Avance III HD, 500.13 MHz for ¹H and 125.8 MHz for ¹³C, BBFO Plus SmartProbe™). Chemical shifts were expressed in ppm (δ) and coupling constants (J) were recorded in (Hz). The TopSpin 4.1 program was used to manipulate the NMR spectra.

The qNMR of the quassinoid fraction based on the PULCON method was evaluated using the ERETIC2 (Electronic Referencing to Access In Vivo Concentrations) tool in TopSpin 4.1 software (Tyburn & Coutant, 2016). The pulse sequence used was the zg90, with time-domain data points (TD) of 64 k, spectral width (SWH) of 10 kHz, relaxation delay (D1) of 20.7 seconds, acquisition time (AQ) of 3.27 seconds, 16 scan numbers (NS) with DS of 2, decomposition resolution of 0.30 Hz,

receiver gain constant at 32 with offset frequency set to 3088, 30 Hz. The calibration pulse (P1 10.313 μ s) was generated with PLW9 of 7.183.10⁻⁵ W. The estimated value of D1 (20.7 s) was seven times the value of T1 for the isobrucein B quassinoid signal (6.03 ppm). Baselines and phases of the samples' 1H NMR spectra were automatically corrected using TopSpin 4.1.

The quantification of the quassinoid fraction was performed in triplicate and consisted of preparing an aliquot (10.1 mg) solubilized in 550 mL of MeOD with TMS as a reference standard (0.0 ppm). The lengths of the 90° pulse were 10.313 μ s of the signals of neosergeolide (δ 5.75) and isobrucein (δ 6.03) and were quantified using the PULCON method. The standard quinine solution (98.0% purity) was prepared (n=3) in concentrations of 13.66 mM in CD₃OD, with TMS as an internal reference (0.0 ppm). The lengths of the 90° pulse were 9.976 μ s of the doublet in 8.65 ppm of quinine. The longitudinal relaxation constant (T1) of the hydrogens of each of the two quassinoids and the quinine to be quantified were determined using the inversion recovery experiment (t1r1d). The measured acquisitions of quinine were 17.11 s (> 7xT1).

2.7 Molecular docking studies of quassinoids and targets of SARS-CoV-2

2.7.1 Chemical structures

The 2D structures of isobrucein B and neosergeolide were drawn on *Chemdraw Ultra* v.12.0. The structure's SMILES were obtained using the interface of the website <http://swissadme.ch/>. The 2D structures were imported to *Discovery Studio Visualizer* v.20 for the obtention of the 3D structures. The same procedure was done for the SARS-CoV-2 3CLpro and RdRp inhibitors, namely X77 and theaflavin, respectively.

2.7.2 Pharmacokinetic predictions

The pharmacokinetic properties and drug-likeness predictions of the quassinoids were performed using SwissADME (Daina et al, 2017) from the structure's SMILES. Predictions included an evaluation of the following parameters: Lipinski's rule of five (molecular weight – MW; hydrogen bond acceptor - HBA; hydrogen bond donor - HBD; and octanol/water partition coefficient - LogP) and several other parameters/properties such as molecular polar surface area (TPSA), logarithm of solubility (LogS), gastrointestinal (GI) absorption, and blood–brain barrier (BBB) permeation. The same calculations were performed with X77 and theaflavin to compare the pharmacokinetic predictions with the SARS-CoV-2 inhibitors.

2.7.3 Toxicity predictions

The compound's toxicity was predicted using the pKCSM (Pires et al., 2015), AdmetSAR (Cheng et al., 2012), Pred-hERG (Braga et al., 2015), and Pred-Skin (Braga et al., 2017) computational tools based on the structure's SMILES. For this purpose, several toxicological parameters were considered, namely Ames toxicity, carcinogenicity, hERG inhibition, skin sensitization, and hepatotoxicity. The results were expressed as "-" for non-detected or "+" for detected risk. The same calculations were performed with X77 and theaflavin.

2.7.4 Docking simulations - Ligand preparation

The 3D structures obtained for the compounds were subjected to geometry optimization by the Dreiding-like forcefield (Hahn, 1995) method in *Discovery Studio Visualizer* v.20, and the results were saved in *Protein Data Bank* (PDB) format.

2.7.5 Protein preparation

The 3D crystal structures of the SARS-CoV-2 3CLpro (PDB: 6W63) and RdRp (PDB: 6M71) were retrieved from Research Collaboratory for Structural Bioinformatics *Protein Data Bank* (RCSB PDB) (<http://www.rcsb.org>) in PDB format. These structures were prepared using *Discovery Studio Visualizer* v.20 tools. Water molecules and bound ligands were removed,

polar hydrogens and Kollman charges were added, and the non-polar hydrogens were merged, and the results were saved in PDB format. *Pymol* v.2.3.4. was then used to visualize the docking results.

2.7.6 Docking calculations

Docking simulations of compounds with SARS-CoV-2 3CLpro and RdRp structures were performed using the *DockThor* server. For 3CLpro, the grid box was centered at $x = -20.810$, $y = 19.141$ and $z = -29.186$, with $x = 24 \text{ \AA}$, $y = 24 \text{ \AA}$ and $z = 24 \text{ \AA}$ size. For RdRp, the grid box was centered at the $x = 117.382$, $y = 111.853$ and $z = 121.073$, with $x = 24 \text{ \AA}$, $y = 24 \text{ \AA}$ and $z = 24 \text{ \AA}$ size. The most energetically favorable conformations were selected for the analysis. The advanced options were maintained as default. The docking protocol was validated by redocking the ligand X77 complexed with the 3CLpro structure. Validation was considered successful if the 10 top-ranked redocked orientations showed heavy atom RMSD values ≤ 2.0 when compared with crystallographic orientation. Due to the lack of models with ligands for RdRp in the RCSB PDB, only the 3CLpro was tested for redocking.

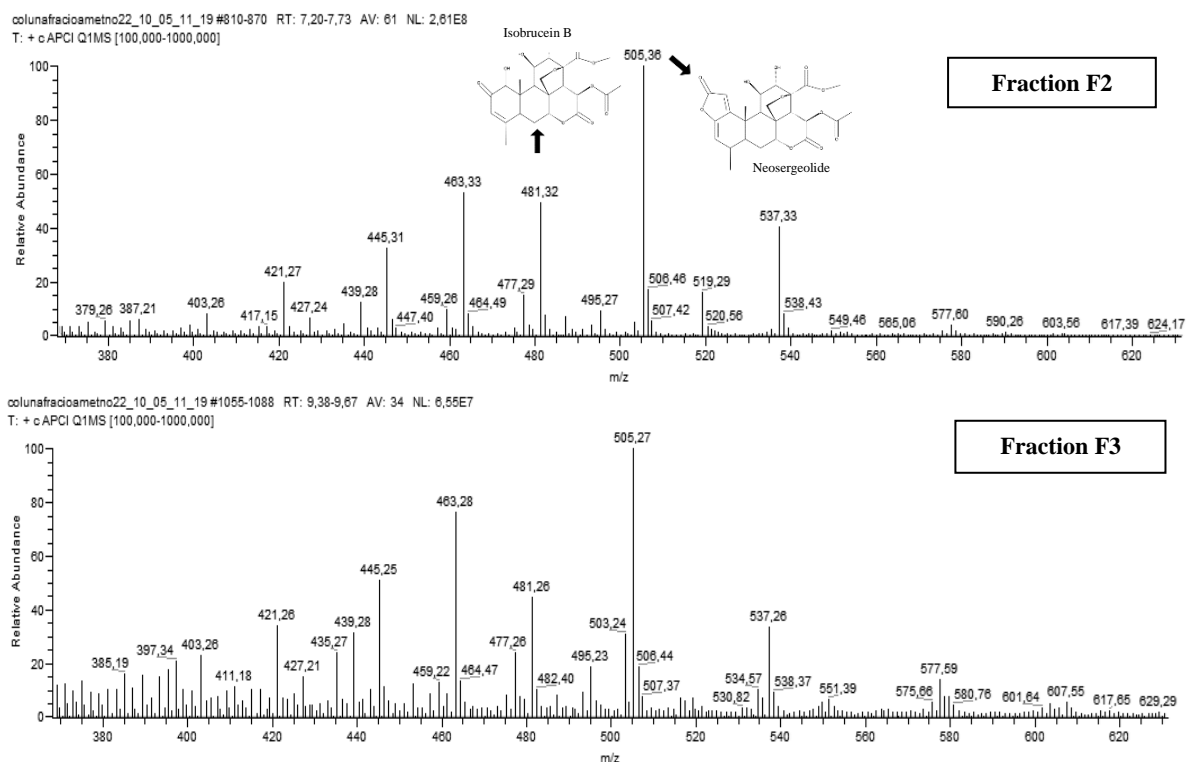
2.8 Statistical analysis

The quantitative NMR data value were compared using the T-test for single comparison and ANOVA (one-way) with a Tukey test (95 % confidence) for multiple comparison using the Minitab[®] 18.1 program (State College, PA, USA), for which the results were expressed as mean \pm standard deviation.

3. Results and Discussion

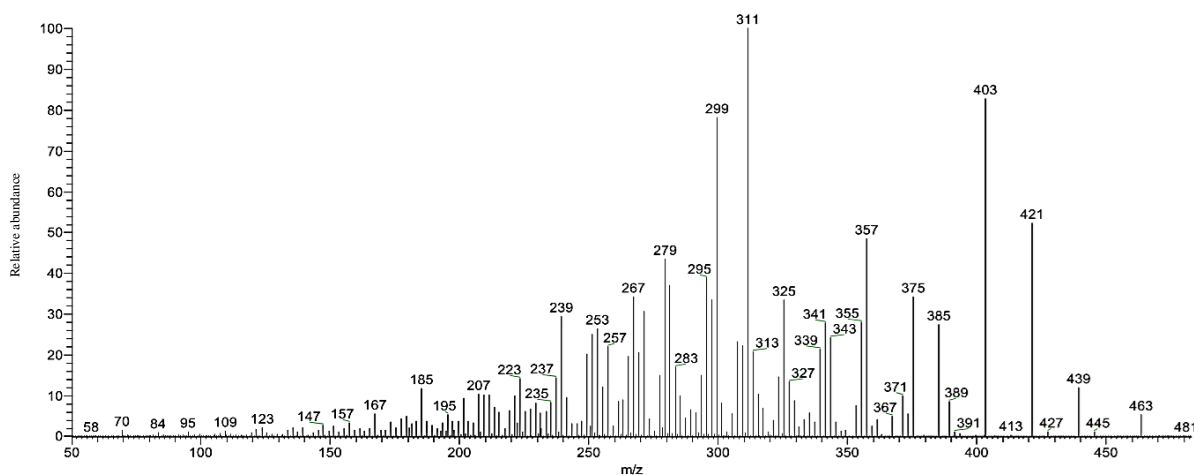
After the complete drying of the PsMeOH extract, its weight was 10.4g with a yield of 3.4% for the mass of plant material (302.54 g). The spectrometric analysis (Figure 1) of the fractions obtained from the extract fractionation column revealed ions referring to the quassinoids isobrucein B at m/z 481 ($[M+H]^+$) and neosergeolide at m/z 505 ($[M+H]^+$) only in fractions F2 and F3. Saraiva (2001) and Amorim (2009) isolated the same known quassinoids from the root of *P. sprucei* for the species under study. Figure 2 presents the fragmentation spectrum (MS/MS) of isobrucein B, and Figure 3 shows the fragmentation spectrum (MS/MS) of neosergeolide, which corroborates the results described by Pohlit (2009). By presenting the profiles in similar mass spectra, the F2 and F3 fractions were pooled, resulting in a weight of 0.7696 g.

Figure 1. Mass spectra of fractions F2 and F3 from the fractionation column of the PsMeOH extract.



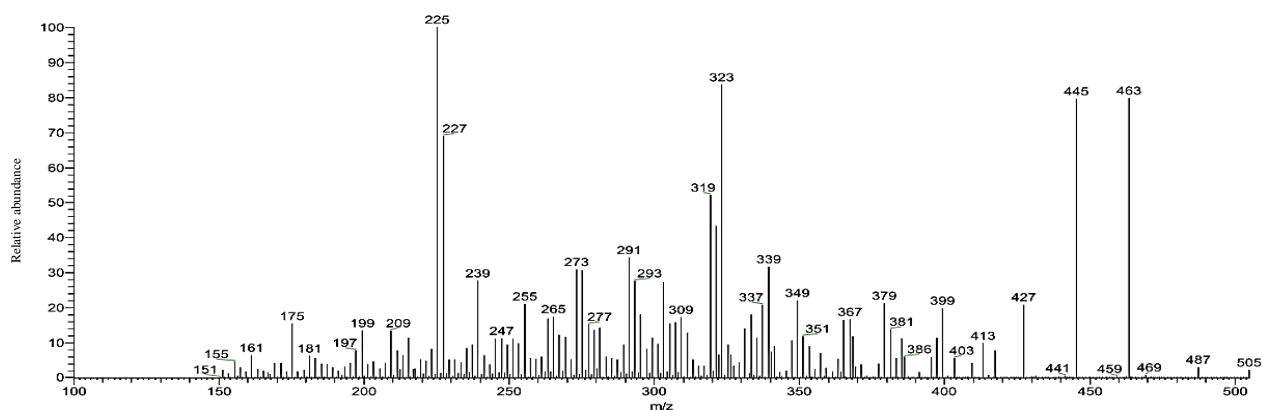
Source: Authors (2021).

Figure 2. MS/MS spectrum of ion m/z 481 ($[M+H]^+$), isobrucein B, present in fractions F2 and F3.



Source: Authors (2021).

Figure 3. MS/MS spectrum of ion m/z 505 ($[M+H]^+$), neosergeolide, present in fractions F2 and F3.

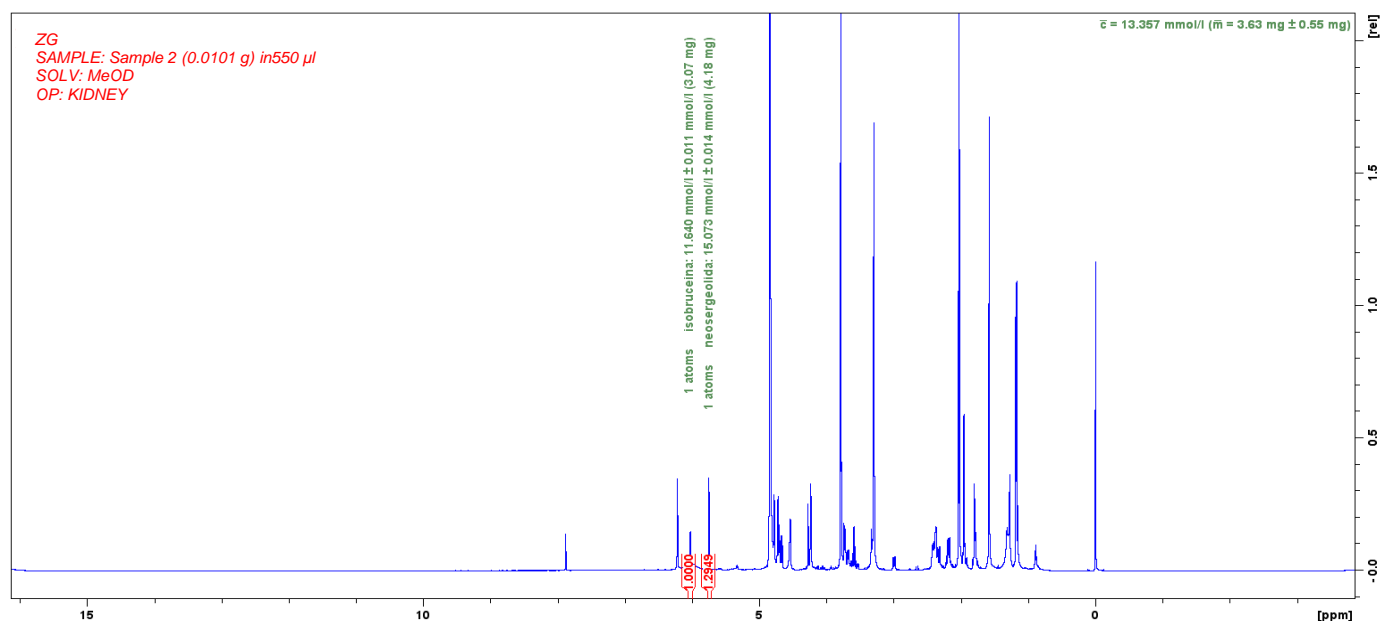


Source: Authors (2021).

The PULCON method correlates absolute intensities of two different spectra and using the principle of reciprocity, which indicates that pulse lengths are inversely proportional to the intensity of the NMR signal, and the analyte concentration is determined (Burton et al, 2005).

The quantitative data obtained by PULCON of the F2-F3 fraction (769.6 mg) with the quassinoids isobrucein B-neosergeolide (Figure 4) enabled the analysis of the proportion of the quassinoids neosergeolide (δ 5.75) and isobrucein B (δ 6.03), and it was possible to observe the ratio of 55.9:44.1, respectively. A relative concentration was used as a function of a known compound to determine the mass of each quassinoid in the total mass. Table 1 shows the mass of each quassinoid considering the total mass of the F2-F3 fraction.

Figure 4. Quantitative ^1H NMR spectrum of replica 1 of the isobrucein B-neosergeolide-mixture. Quantification by qNMR was performed for signals δ 5.75 (neosergeolide) and δ 6.03 (isobrucein).



Source: Authors (2021).

Table 1. Mass of each of the quassinoids present in the F2-F3 fraction and the PsMeOH extract.

Compounds	Conc. (mg/mL)	Conc. (mM)	Fraction F2-F3 (%)	PsMeOH extract (%)
Neosergeolide	7.59±0.15 ^a	15.06±0.81 ^a	41.35±0.84 ^a	3.05±0.06 ^a
Isobrucein B	6.01±0.41 ^b	12.51±0.84 ^b	32.71±2.23 ^b	2.41±0.16 ^b
Other compounds	4.76±0.49 ^c	-	25.94±2.69 ^c	1.91±0.20 ^c

Values with the same letter in the same column are not significantly different ($p < 0.05$). Source: Authors (2021).

The quantitative analysis of quassinoids in root-based teas carried out by Nunomura et.al. (2012) provided results different from those presented in this work since ours showed a higher concentration of isobrucein B than neosergeolide. However, it should be considered that since isobrucein B is more polar than neosergeolide, it is possibly better extracted by using water as a solvent. The quantification showed the quassinoids as the most representative compounds present in the PsMeOH extract of the *P. sprucei* roots since the percentage of the two quassinoids adds up to 5.46% of the total mass (10.4 g) of the PsMeOH extract.

Considering that the quassinoids present in the species are potentially active for several biological activities, a theoretical study of these compounds against the proteins of SARS-CoV-2 was carried out. However, being highly bioactive is not a good enough criterion to qualify the compound as a good candidate (Guan et al., 2019). A better pharmacokinetic profile is extremely important for a novel compound examined in the process of drug/drug-like compound discovery. Hence, it is imperative to evaluate the ADMET profile of new compounds earlier to avoid a possible waste of time/resources (Shou, 2020).

The ADMET analysis results revealed the physicochemical properties of the quassinoids and the SARS-CoV-2 3CLpro and RdRp inhibitors, as represented in Table 2. According to Lipinski's rule of five (Lipinski et al., 2001), most of the compounds followed the rules by causing no more than one violation. That is to say, the MW, HBA, HBD, and LogP are within the acceptable range. However, the quassinoids were predicted as having low GI absorption, and thus not good in an orally bioavailable sense, and this may be due to its polar character (LogS and TPSA calculated). Only X77 was predicted as having high GI absorption. On the other hand, none of the compounds were predicted to have BBB permeation. In general, the quassinoids and the SARS-CoV-2 inhibitors possess a good pharmacokinetic profile.

Table 2. Calculated ADME parameters of the quassinoids and SARS-CoV-2 3CLpro and RdRp inhibitors.

Pharmacokinetic parameters	Isobrucein B	Neosergeolide	Theaflavin	X77
MW (g/mol)	480.46	504.48	564.49	459.58
HBA	11	11	12	4
HBD	3	2	9	2
Log P	-0.34	0.81	1.31	3.88
Druglikeness (Lipinski)	Yes (1 violation)	No (2 violations)	No (3 violations)	Yes (0 violation)
Log S	-0.77	-1.36	-4.22	-7.74
TPSA (Å ²)	165.89	154.89	217.60	90.98
GI absorption	Low	Low	Low	High
BBB permeation	No	No	No	No

Key: MW = molecular weight; HBA = hydrogen bond acceptor; HBD = hydrogen bond donor; Log P = octanol/water partition coefficient; Log S = logarithm of solubility; TPSA = Topological polar surface area; GI= Gastrointestinal absorption; BBB= blood-brain barrier. Source: Authors (2021).

The toxicophorical analysis of the compounds was performed with tools that are capable of identifying the main chemical substructures related to toxicity data, thus guiding the design of inhibitors with low toxic potential (Whu & Wang, 2018). This strategy intends to minimize common toxicity failures in the early stages of drug discovery (Rim, 2020). The result of the toxicity analysis of the quassinoids and the SARS-CoV-2 3CLpro and RdRp inhibitors is represented in Table 3. Prediction data revealed no risks regarding carcinogenicity. In contrast, a predicted risk of skin sensitization was attributed to the compounds, which is a potential adverse effect for dermally applied products (Kleinstreuer et al., 2018). Only Neosergeolide and X77 were predicted as non-inhibitors of the hERG channel, for which inhibition may lead to ventricular arrhythmia (Priest et al., 2008). On the other hand, a detected risk of Ames toxicity and hepatotoxicity was predicted for X77. The Ames test is a short-term bacterial reverse test for mutagenicity prediction (Mortelmans & Zeiger, 2000). In general, we can observe that the quassinoids possess lower toxicological potential than the SARS-CoV-2 inhibitors.

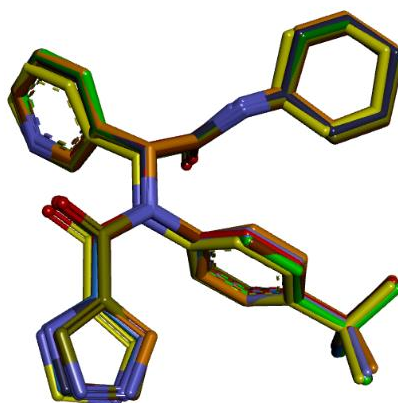
Table 3. Calculated toxicity parameters of the quassinoids and SARS-CoV-2 3CLpro and RdRp inhibitors.

Toxicity parameter	Isobrucein B	Neosergeolide	Theaflavin	X77
Ames toxicity ^{1,2}	-	-	-	+
Carcinogenicity ²	-	-	-	-
hERG inhibition ³	+	-	+	-
Skin sensitization ⁴	+	+	+	+
Hepatotoxicity ¹	-	-	-	+

¹pKCSM ²AdmetSAR ³Pred-hERG ⁴Pred-Skin. Source: Authors (2021).

Molecular docking analysis were performed to verify the conformation of the quassinoids within SARS-CoV-2 targets and the binding affinities. First, the redocking procedure with the ligand X77 complexed in SARS-CoV-2 3CLpro binding site revealed that all the 10-top ranked orientations presented heavy atoms RMSD < 2 when compared with the crystallographic conformation (Figure 5). The docking protocol was able to reproduce the conformation and the binding mode of X77, thus validating our docking simulations.

Figure 5. Superimposition of the crystallographic structure of X77 (carbon atoms in yellow) and the ten top-scored orientations obtained by docking.



Source: Authors (2021).

Docking simulations between the compounds and SARS-CoV-2 3CLpro revealed that they bind at the receptor-binding pocket mainly by hydrogen bond (HB) and Van der Waals interactions (Figure 7 and 8). The compounds presented interactions

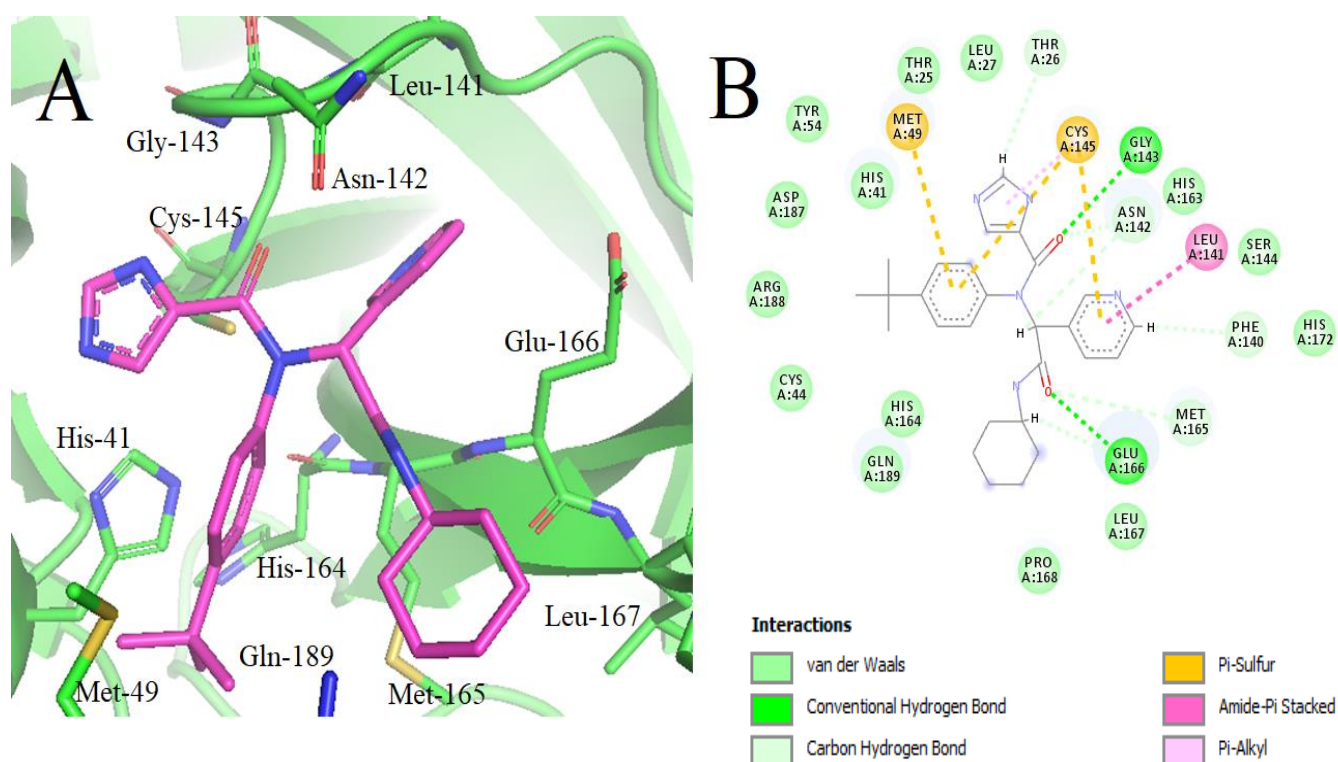
with the receptor residues such as those observed in the inhibitor's binding mode (Figure 6 and Table 4) and are thus capable of interacting with the catalytic dyad (His41 and Cys145) of the receptor (Qamar et al., 2020). The catalytically active 3CLpro is a dimer. Cleavage by 3CLpro occurs in the glutamine residue of the substrate via the protease Cys-145 and His-41 dyad in which the cysteine thiol functions as the nucleophile in the proteolytic process (Anand et al., 2003). Predicted binding affinities showed that, although X77 presented the stronger affinity, the quassinoids showed similar values compared to X77 (Table 4).

Table 4. Predicted binding affinity, intermolecular energies, and key interacting receptor residues of docked poses of isobrucein B, neosergeolide and redocked pose of X77 within SARS-CoV-2 3CLpro binding site.

Ligand	Affinity (kcal/mol)	Van der Waals energy (kcal/mol)	Electrostatic energy (kcal/mol)	Key interacting residues
Isobrucein B	-8.024	-23.019	-5.398	His-41, Asn-142, Cys-145 and Glu-166
Neosergeolide	-8.248	-23.116	-8.630	Glu-166, Ser-144, Cys-145, Gln-189
X77	-9.558	-38.182	-7.684	His-41, Met-49, Leu-141, Gly-143, Cys-145, Glu-166

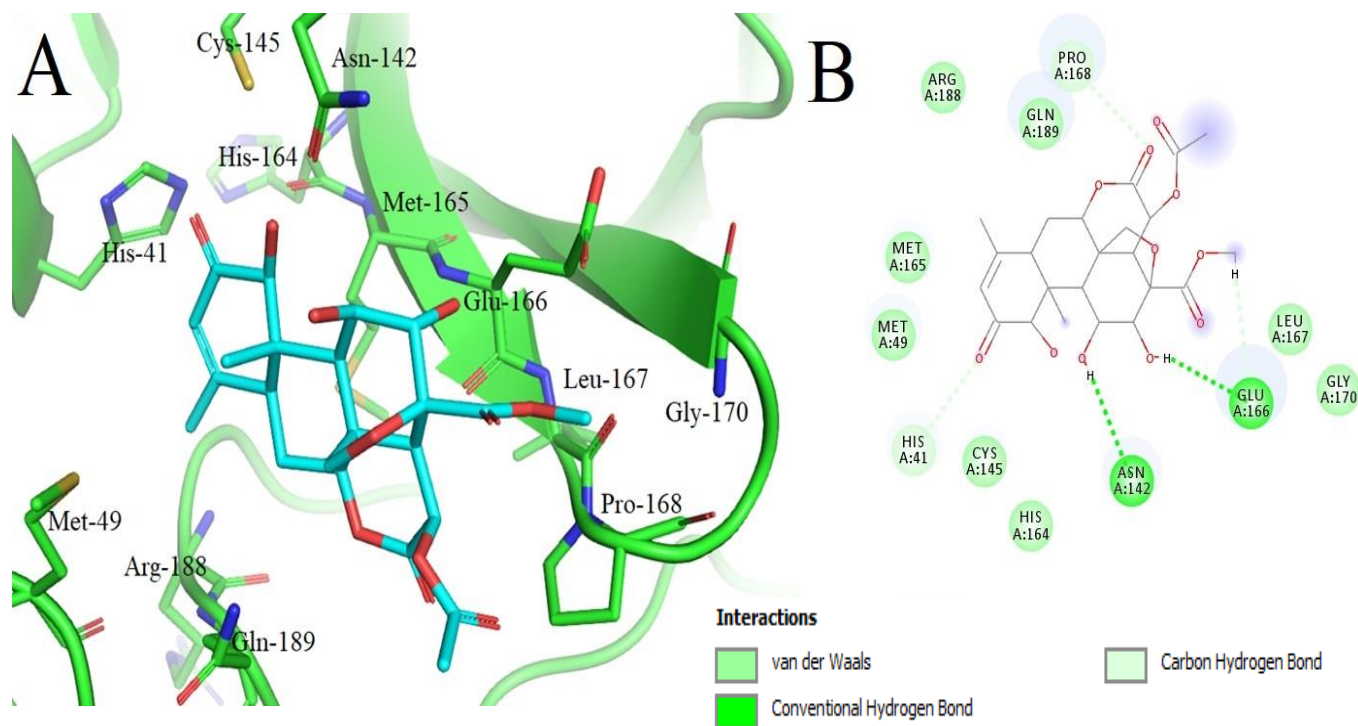
Source: Authors (2021).

Figure 6. (A) 3D docking model of X77 (carbon atoms in purple) within the SARS-CoV-2 3CLpro binding site, highlighting the main intermolecular interactions with residues. (B) 2D interaction diagram between the X77 and receptor residues.



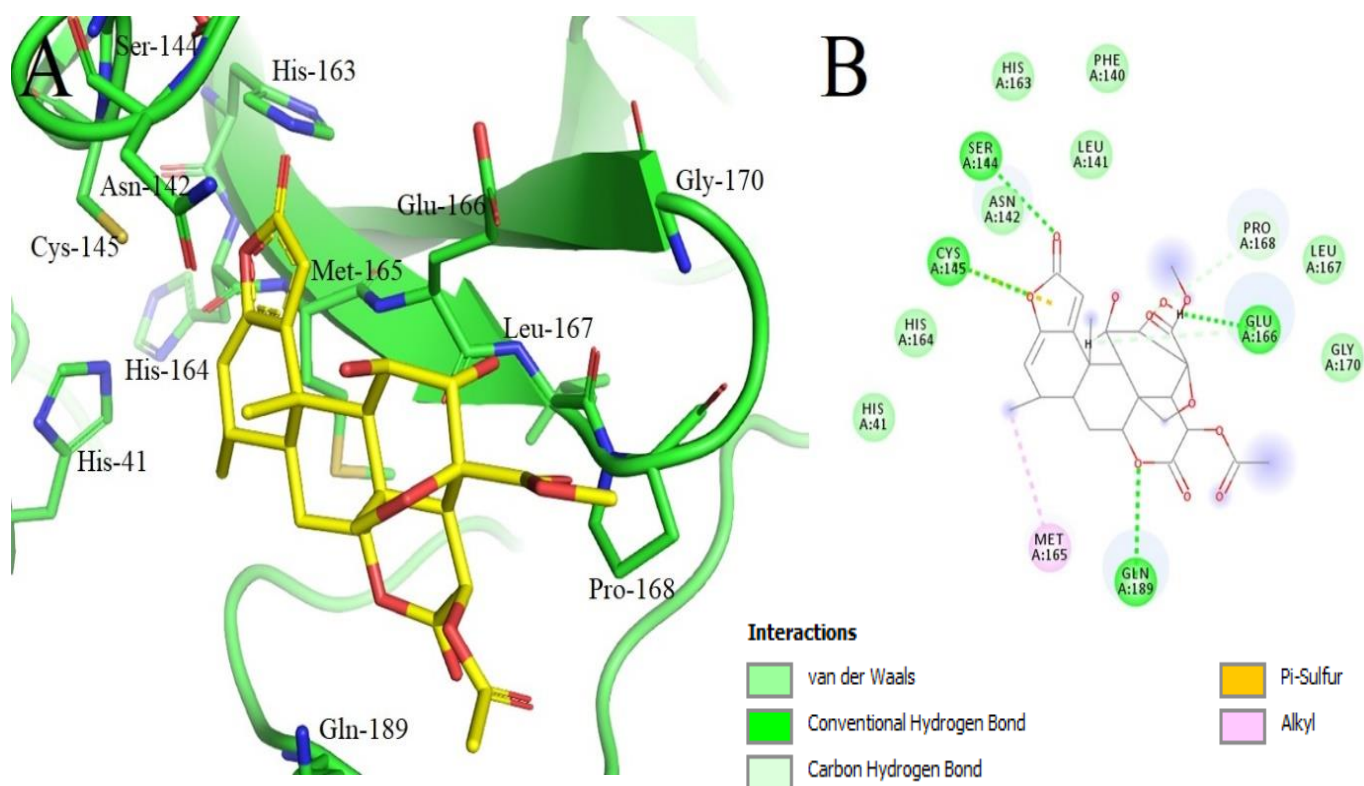
Source: Authors (2021).

Figure 7. (A) 3D docking model of isobrucein B (carbon atoms in cyan) within the SARS-CoV-2 3CLpro binding site, highlighting the main intermolecular interactions with residues. (B) 2D interaction diagram between the isobrucein B and receptor residues.



Source: Authors (2021).

Figure 8. (A) 3D docking model of neosergeolide (carbon atoms in yellow) within SARS-CoV-2 3CLpro binding site, highlighting the main intermolecular interactions with residues. (B) 2D interaction diagram between the neosergeolide and receptor residues.



Source: Authors (2021).

Docking simulations with SARS-CoV-2 RdRp revealed that the quassinoids may bind at the nucleoside triphosphates (NTP) binding pocket. This active site includes motif A (residues 611-626), with the classic divalent cation-binding residue 618, and motif C (residues 753-767), with the catalytic residues 759-761 (Gao et al., 2020). The compounds isobrucein B, neosergeolide and theaflavin performed interactions with these key residues mainly by HB, Van der Waals, and Pi interactions (Figure 9-11). The binding across the RNA tunnel potentially blocks the access of NTPs to the active site on one side and of RNA on the other. Without NTPs, RNA replication cannot occur, thus blocking viral replication (Pokhrel et al 2020). The binding affinities of the compounds with the receptor were similar when compared to the values obtained for theaflavin (Table 5).

Table 5. Predicted binding affinity, intermolecular energies, and key interacting receptor residues of docked poses of isobrucein B, neosergeolide and theaflavin within the SARS-CoV-2 RdRp binding site.

Ligand	Affinity (kcal/mol)	Van der Waals energy (kcal/mol)	Electrostatic energy (kcal/mol)	Key interacting residues
Isobrucein B	-7.500	-11.971	-26.312	Lys-551, Asp-618, Lys-798, Trp-800 and Glu-811
Neosergeolide	-7.388	-21.629	-17.490	Arg-553, Asp-618, Tyr-619, Lys-621, Asp-761,
theaflavin	-7.671	-8.245	-52.988	Arg-553, Asp-618, Asp-623, Asp-760, Asp-761 and Lys-798

Source: Authors (2021).

Figure 9. (A) 3D docking model of isobrucein B (carbon atoms in cyan) within the SARS-CoV-2 RdRp binding site, highlighting the main intermolecular interactions with residues. (B) 2D interaction diagram between isobrucein B and the receptor residues.

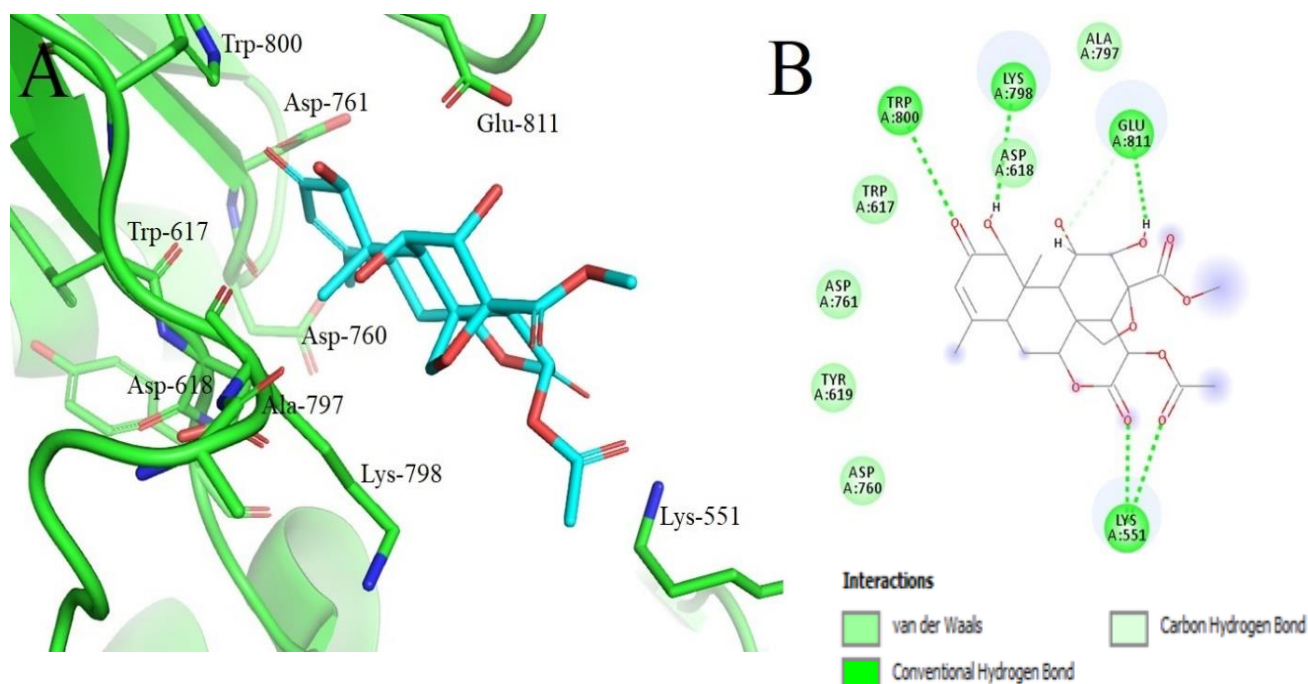


Figure 10. (A) 3D docking model of neosergeolide (carbon atoms in yellow) within the SARS-CoV-2 RdRp binding site, highlighting the main intermolecular interactions with residues. (B) 2D interaction diagram between neosergeolide and the receptor residues.

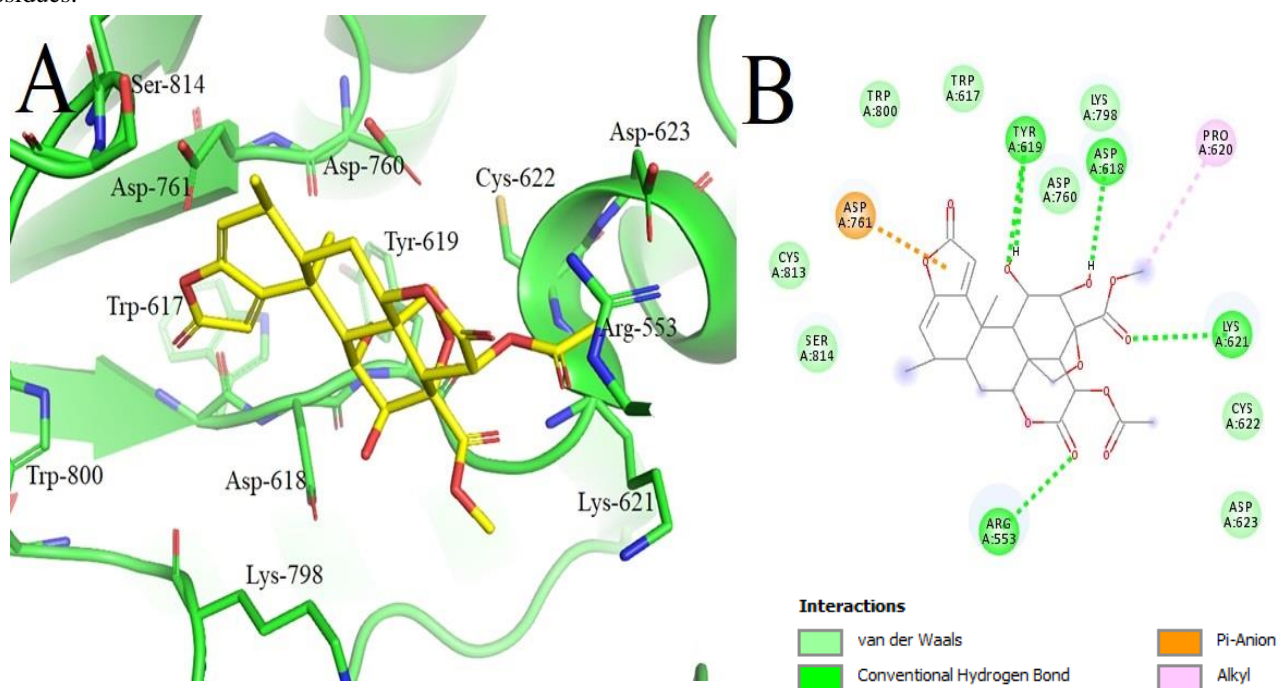
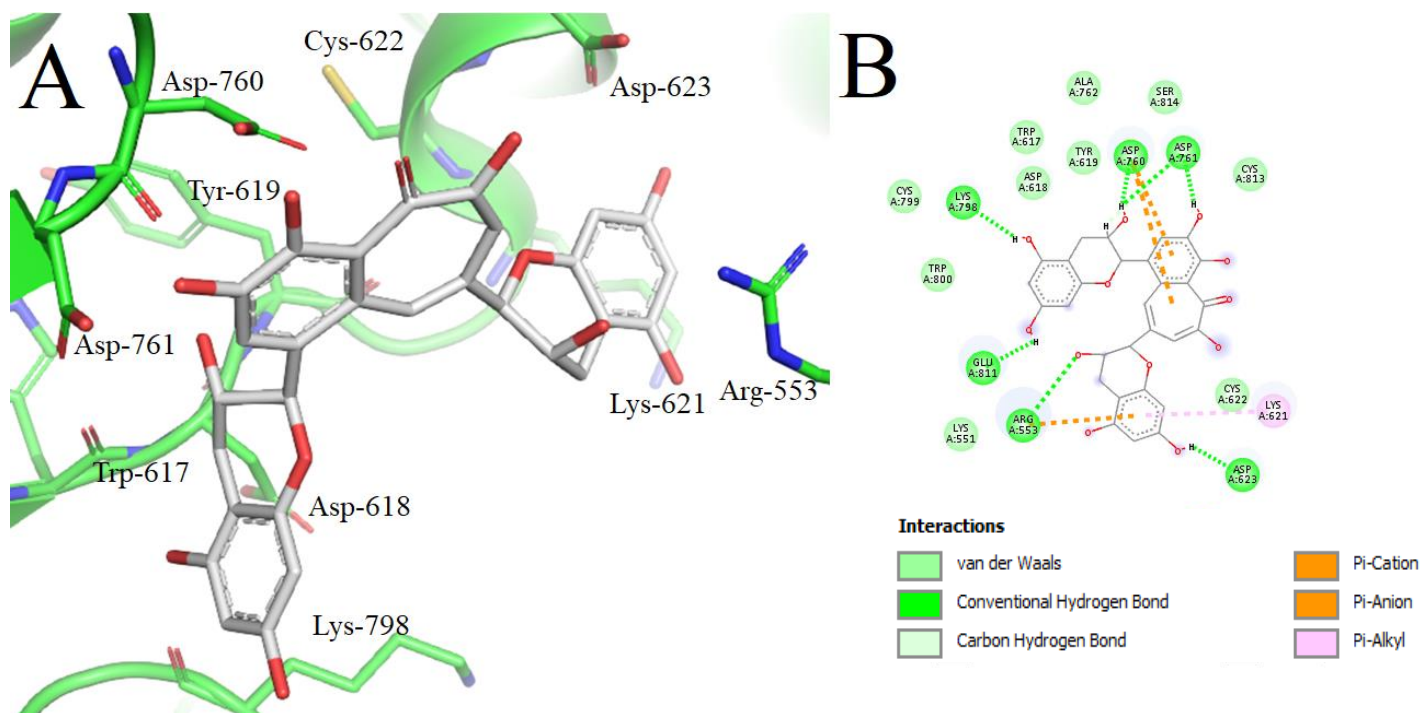


Figure 11. (A) 3D docking model of theaflavin (carbon atoms in gray) within the SARS-CoV-2 RdRp binding site, highlighting the main intermolecular interactions with the residues. (B) 2D interaction diagram between theaflavin and the receptor residues.



Source: Authors (2021).

Molecular modeling, including several *in silico* experiments, has become an essential tool for the planning and development of drugs for various diseases. A series of comparative evaluations of docking programs carried out over the past few years have indicated that the programs, as well as the molecular docking method, can generate binding forms that are like those already experimentally determined and that have already been published in the literature (Zaheer-ul-haq et al., 2010). The results of the molecular docking simulations in this work propose the quassinoids' capacity to interact with key amino acids residues in SARS-CoV-2 targets, which shows the potential of isobrucein B and neosergeolide as possible inhibitors of the SARS-CoV-2 target proteins 3CLpro and RdRp. Few molecular docking studies using quassinoids and SARS-Cov-2 have been reported, and no studies using quassinoids from *P. sprucei* and SARS-CoV-2 have been reported yet. Some studies have shown that compounds of natural origin have potential SARS-CoV-2 inhibitors.

Rahmatullah et al. (2020) carried out a molecular docking study with the 3CLpro protein from SARS-CoV-2 with 12 Javanicins, which are quassinoids found in the *Picrasma javanica* species from the Simaroubaceae family. The quassinoid Javanicin G showed the greatest affinity for SARS-CoV-2 3CLpro with a binding energy of -8.2 kcal/mol. This result found by these authors corroborates the result found for neosergeolide and 3CLpro protein, in which neosergeolide also presented an affinity of 8.248 kcal/mol.

Hasan et al. (2020) reported the interaction of 7 quassinoid javanicolides found in *Brucea javanica* with 3CLpro. Javanicolide B showed a higher affinity for 3CLpro with a binding energy of -7.9 kcal/mol. Pele et al. (2020) evaluated some antimalarial compounds of natural origin for SARS-CoV-2 3CLpro. In the study, the following antimalarials quinine, primaquine, atovaquone, artesunate, and proguanil presented binding affinity values -6.508 kcal/mol, -6.361 kcal/mol, -5.493 kcal/mol, -4.862 kcal/mol, and -4.842 kcal/mol, respectively. These values are lower than the quassinoids isobrucein B and neosergeolide, for which the binding affinity value was -8.024 kcal/mol and -8.248 kcal/mol for this target.

Guedes et al. (2021) evaluated the repositioning of drugs using the SARS-CoV-2 3CLpro and RdRp targets. These drugs are already used in clinical practice and were analyzed against the SARS-CoV-2 targets mentioned above. Some of these drugs had a binding affinity value for 3CLpro and RdRp that was lower than the quassinoids studied in this work, bearing in mind that the more negative (and further from zero) the value of ΔG° , the more affinity the ligand has for the target. Some antimalarial drugs, such as chloroquine, hydroxychloroquine, and mefloquine, had values of -8.06 kcal/mol, -7.83 kcal/mol, and -7.46 kcal/mol, respectively for the 3CLpro target. In contrast, the quassinoid neosergeolide showed a higher affinity with a value of -8.248 kcal/mol for the same target. Isobrucein B had greater affinity than the values shown by hydroxychloroquine and mefloquine, and a value close to the value of chloroquine with a binding affinity value of -8.024 kcal/mol.

As for the RdRp target of SARS-CoV-2 in the same study by Guedes et al. (2021), the binding affinity values for the drugs chloroquine, hydroxychloroquine, and mefloquine were -7.49 kcal/mol, -7.42 kcal/mol, and -7.03 kcal/mol, respectively. Isobrucein B had a binding affinity value of -7.500 kcal/mol, slightly higher than those of chloroquine and hydroxychloroquine, and a higher binding affinity for the RdRp target than mefloquine. For this target, the quassinoid neosergeolide had an affinity value a little lower than that of chloroquine and hydroxychloroquine and greater than the value of mefloquine, with a binding affinity of -7.388 kcal/mol.

4. Conclusion

Using the qNMR technique, which until now had not been used for the quassinoids of the species *P. sprucei*, it was possible to quantify them in the F2-F3 fraction. The *in silico* results suggest that the quassinoids isobrucein B and neosergeolide are interesting starting points for obtaining novel SARS-CoV-2 inhibitors with therapeutic potential in the treatment of COVID-19. This is the first study of the binding of *P. sprucei* quassinoids (by molecular docking) to key proteins of SARS-CoV-2 that play an important role in inhibiting virus replication. Thus, these two quassinoids may play an essential role as inhibitors of SARS-CoV-2 3CLpro and RdRp.

Analyses *in vitro* and *in vivo* are needed to corroborate the reported docking results and the proper application and further optimization of these substances. The knowledge obtained in this study may be essential for exploring and developing new candidates for natural therapeutic agents against COVID-19. Furthermore, it is also fundamental that we investigate the risks of *P. sprucei* as a phytomedicine for use against COVID-19.

Acknowledgments

The authors would like to thank the Financiadora de Estudos e Projetos - FINEP, Fundação de Amparo à Pesquisa do Estado do Amazonas - FAPEAM and Coordenação de Aperfeiçoamento de Pessoal de Nível Superior - CAPES and the Programa de Pós-graduação em Inovação Farmacêutica of UFAM and Central Analítica at UFAM for the use of its infrastructure, its financial support and internships.

References

- Amorim, R. C. N. (2009). Contribuições para o conhecimento da composição química e atividade biológica de infusões, extratos e quassinóides obtidos de *Picrolemma sprucei* Hook.f. (Simaroubaceae). Tese de Doutorado em Biotecnologia - Universidade Federal do Amazonas, Manaus, AM, Brasil.
- Anand, K., Ziebuhr, J., Wadhwani, P., Mesters, J. R. & Hilgenfeld, R. (2003). Coronavirus Main Proteinase (3CLpro) Structure: Basis for Design of Anti-SARS Drugs. *Science*, 300, 1763–1767.
- Andrade-Neto, V. F., Pohlit, A. M., Pinto, A. C. S., Silva, E. C. C., Nogueira, K. L., Melo, M. R. S., Henrique, M. C., Amorim, R. C. N., Silva L. F. R. & Costa, M. R. F. (2007). *In vitro* inhibition of *Plasmodium falciparum* by substances isolated from Amazonian antimalarial plants. *Memórias do Instituto Oswaldo Cruz*, 102(3), 359–366.

- Beyer, T., Schollmayer, C., Holzgrabe, U. (2010). The role of solvents in the signal separation for quantitative ^1H NMR spectroscopy. *Journal of pharmaceutical and biomedical analysis*, 52, 51–58.
- Braga, R. C., Alves, V. M., Muratov, E. N., Strickland, J., Kleinstreuer, N., Tropsha, A. & Andrade, C. H. J. (2017). Pred-Skin: A Fast and Reliable Web Application to Assess Skin Sensitization Effect of Chemicals. *Journal of Chemical Information and Modeling*, 57 (5), 1013–1017.
- Braga, R. C., Alves, V. M., Silva, M. F. B., Muratov, E., Fourches, D., Liao, L. M., Tropsha, A. & Andrade, C. H. (2015). Pred-hERG: A novel web-accessible computational tool for predicting cardiac toxicity. *Molecular Informatics*, 34, 698-701.
- Burton, I. W., Quilliam, M. A. & Walter, J. A. (2005). Quantitative ^1H NMR with external standards: use in preparation of calibration solutions for algal toxins and other natural products. *Analytical Chemistry*, 77, 3123–3131.
- Cheng, F., Li, W., Zhou, Y., Shen, J., Wu, Z., Liu, G., Lee, P.W. & Tang, Y. (2012). AdmetSAR: a comprehensive source and free tool for assessment of chemical ADMET properties. *Journal of Chemical Information and Modeling*, 52, 3099–3105.
- Daina, A., Michielin, O. & Zoete, V. (2017). SwissADME: a free web tool to evaluate pharmacokinetics, drug-likeness and medicinal chemistry friendliness of small molecules. *Scientific Reports*, 7, 42717.
- Das, S., Sarmah, S., Lyndem, S. & Roy, A. S. (2020). An investigation into the identification of potential inhibitors of SARS-CoV-2 main protease using molecular docking study. *Journal of Biomolecular Structure and Dynamics*, 1-11.
- Da Silva, F. M. A., da Silva, K. P. A., de Oliveira, L. P. M., Costa, E. V., Koolen, H. H. F., Pinheiro, M. L. B., de Souza, A. Q. L. & de Souza, A. D. L. (2020). Flavonoid glycosides and their putative human metabolites as potential inhibitors of the SARS-CoV-2 main protease (Mpro) and RNA-dependent RNA polymerase (RdRp). *Mem. Inst. Oswaldo Cruz*, 115, 1–8.
- Dong, E., Du, H. & Gardner, L. (2020). An interactive web-based dashboard to track COVID-19 in real time, *Lancet Infectious Diseases*, 20(5), 533-534.
- Ferreira, M. C. (2000). O mercado de plantas medicinais em Manaus. In: A floresta em jogo. O extrativismo na Amazônia Central. Editor: L' Orstom. Editora científica Laure Empereire, tradução brasileira Editora da UNESP, 177-181.
- Fukamiya, N., Lee, K. H., Muhammad, I., Murakami, C., Okano, M., Harvey, I., Pelletier, J. (2005). Structure-activity relationships of quassinoids for eukaryotic protein synthesis. *Cancer Letter*, 220, 37-48.
- Gao, Y., Yan, L., Huang, Y., Liu, F., Zhao, Y., Cao, L., Wang, T., Sun, Q., Ming, Z., Zhang, L., Ge, J., Zheng, L., Zhang, Y., Wang, H., Zhu, Y., Zhu, C., Hu, T., Hua, T., Zhang, B., Yang, X., Li, J., Yang, H., Liu, Z., Xu, W., Guddat, L. W., Wang, Q., Lou, Z. & Rao, Z. (2020). Structure of the RNA-dependent RNA polymerase from COVID-19 virus. *Science*, 368(6492), 779-782.
- Ghahremanpour, M. M., Tirado-Rives, J., Deshmukh, M., Ippolito, J. A., Zhang, C.H., Vaca, I.C., Liosi, M. E., Anderson, K. S. & Jorgensen, W. L. (2020). Identification of 14 known drugs as inhibitors of the main protease of SARS-CoV-2. *ACS Medicinal Chemistry Letters*, 11(12), 2526-2533.
- Guan, L., Yang, H., Cai, Y., Sun, L., Di, P., Li, W., Liu, G. & Tang, Y. (2018). ADMET- score - a comprehensive scoring function for evaluation of chemical drug-likeness. *Medchemcomm*, 10(1), 148-157.
- Guedes, I. A., Costa, L. S. C., Santos, K. B., Karl, A. L. M., Rocha, G. K., Teixeira, I. M., Galheigo, M. M., Medeiros, V., Krempser, E., Custódio, F. L., Barbosa, H. J. C., Nicolás, M. F. & Dardeme L. E. (2021). Drug design and repurposing with DockThor-VS web server focusing on SARS-CoV-2 therapeutic targets and their non-synonym variants. *Scientific Reports*, 11, 5543.
- Guo, Z., Vangapandu, S., Sindelar, R.W., Walker, L.A. & Sindelar, R. D. (2005). Biologically active quassinoids and their chemistry: Potential leads for drug design. *Current Medicinal Chemistry*, 12, 173-190.
- Hahn, M. Receptor Surface Models. 1. Definition and Construction. (1995). *Journal of Medicinal Chemistry*, 38, 12, 2080–2090.
- Hasan, A., Mahamud R. A., Bondhon, T. A., Jannat, K., Jahan, R., Rahmatullah M. (2020). Can javanicins be potential inhibitors of SARS-CoV-2 C-3 like protease? An evaluation through molecular docking studies. *Journal of Natural & Ayurvedic Medicine*, 4(2), 000250.
- Hasan, A., Mahamud, R. A., Bondhon, T. A., Jannat, K., Farzana, B., Jahan & Rahmatullah, M. (2020). Molecular docking of quassinoid compounds javanicolides A-F and H with C3-like protease (or 3CL pro) of SARS and SARS-C0V-2 (COVID-19) and VP8* domain of the outer capsid protein VP4 of rotavirus A. *Journal of Medicinal Plants Studies*. 2020; 8(4 Part A):14-19.
- Kleinstreuer, N. C., Hoffmann, S., Alépée, N., Allen, D., Ashikaga, T., Casey, W., Clouet, E., Cluzel, M., Desprez, B., Gellatly, N., Göbel, C., Kern, P. S., Klaric, M., Kühnl, J., Martinuzzi-Teissier, S., Mewes, K., Miyazawa, M., Strickland, J., van Vliet, E., Zang, Q. & Petersohn D. Non-animal methods to predict skin sensitization (II): an assessment of defined approaches*. *Critical Reviews in Toxicology*, 48(5), 359-374.
- Le Cointe, P. (1947). Árvores e plantas úteis (Amazônia brasileira III). Companhia Editora Nacional, 92.
- Lipinski, C. A., Lombardo, F., Dominy, B. W. & Feeney, P.J. (1997). Experimental and Computational Approaches to Estimate Solubility and Permeability in Drug Discovery and Development Settings. *Advanced Drug Delivery Reviews*, 23, 3-25.
- Moretti, C., Polonsky, J., Vuilhorgne, M. & Prange, T. Isolation and structure of sergeolide a potent cytotoxic quassinoid from *Piccolema pseudocoffea*. *Tetrahedron Letters*, 23(6), 647-650, 1982.
- Morse, J. S., Lalonde, T., Xu, S. & Liu, W. R. (2020) Learning from the past: possible urgent prevention and treatment options for severe acute respiratory infections caused by 2019-nCoV. *ChemBioChem*, 21(5), 730-738.
- Mortelmans, K. & Zeiger E. The Ames Salmonella/microsome mutagenicity assay. (2000). *Mutation Research*, 20;455(1-2):29-60.

- Neves, K. O. G., Ramos, A. S., Bruginski, E. R. D., De Souza, A. D. L., Nunomura, R. C. S., Campos, F. R., Da Silva, F. M. A. & Machado, M. B. (2021). Lisboaeflavanonol A: A new flavonoid glycoside obtained from Amazonian *Eugenia lisboae*. *Phytochemistry Letters*, 43, 65-69.
- Nunomura, R. C. S., Silva, E. C. C., Oliveira, D. F., Garcia, A. M., Boeloni, J. N., Nunomura S. M. & Pohlit, A. M. (2006). *In vitro* studies of the anthelmintic activity of *Picrolemma sprucei* Hook. f. (Simaroubaceae). *Acta Amazonica*, 36, 327-330.
- Nunomura, R. C. S., Silva, E. C. C., Nunomura, S. M., Amaral, A. C. F., Barreto, A. S., Siani A. C., Pohlit, A. M. (2012). Quantification of antimalarial quassinoids neosergeolide and isobrucein b in stem and root infusions of *Picrolemma sprucei* Hook F. by HPLC-UV analysis. *Chromatography and Its Applications*, 187-200.
- Oliveira, E. S. C., Pontes, F. L. D., Acho, L. D. R., do Rosário, A. S., da Silva, B. J. P., de A Bezerra, J., Campos, F. R., Lima, E. S. & Machado, M. B. (2021). qNMR quantification of phenolic compounds in dry extract of *Myrcia multiflora* leaves and its antioxidant, anti-AGE, and enzymatic inhibition activities. *Journal of Pharmaceutical and Biomedical Analysis*, 15, 201:114109.
- Peele, K. A., Potla, D. C., Srihansa, T., Krupanidhi, S., Ayyagari, V. S., Babu, D. J., Indira, M., Reddy, A. R., & Venkateswarulu T. C. (2020). Molecular docking and dynamic simulations for antiviral compounds against SARS-CoV-2: a computational study. *Informatics in Medicine Unlocked*, 19, 100345.
- Pires, D. E., Blundell, T. L. & Ascher, D. B., (2015). pkCSM: predicting small-molecule pharmacokinetic and toxicity properties using graph-based signatures. *Journal of Medicinal Chemistry*, 58, 4066-4072.
- Pohlit, A. M., Jabor, V. A. P., Amorim, R. C. N., Silva, E. C. C. & Lopes, N. P. (2009). LC-ESI-MS Determination of quassinoids isobrucein B and neosergeolide in *Picrolemma sprucei* stem infusions. *Journal of the Brazilian Chemical Society*. 20(6), 1065-1070.
- Pokhrel, R., Chapagain, P. & Siltberg-Liberles, J. (2020). Potential RNA-dependent RNA polymerase inhibitors as prospective therapeutics against SARS-CoV-2. *Journal of Medical Microbiology*, 69(6), 864-873.
- Priest, B. T., Bell, I. M. & Garcia, M. L. (2008). Role of hERG potassium channel assays in drug development. *Channels (AUSTIN)*, 2(2), 87-93.
- Qamar, M. T., Alqahtani, S. M., Alamri, M. A. & Chen, L. L. (2020). Structural basis of SARS-CoV-2 3CLpro and anti-COVID-19 drug discovery from medicinal plants. *Journal of Pharmaceutical Analysis*, 10(4), 313-319.
- Ribeiro, J. E. L.; Hopkins, M. J. G.; Vicentini, A.; Sothers, C. A.; Costa, M. A. S.; Brito, J. M.; Souza, M. A. D.; Martins, L. H. P.; Lohmann, L. G.; Assunção, P. A. C. L.; Pereira, E. C.; Silva, C. F.; Mesquita, M. R.; Procópio, L. C. (1999). Flora da Reserva Ducke – Guia de identificação das plantas vasculares de uma floresta de terra-firme na Amazônia Central. Manaus-AM, INPA, p. 547-549.
- Rim, K. T. (2020). *In silico* prediction of toxicity and its applications for chemicals at work [published online ahead of print, 2020 May 14]. *Toxicol Environ Health Sci*, 1-12.
- Saraiva, R. C. G. (2001). Estudo Fitoquímico de *Picrolemma sprucei* Hook (Simaroubaceae) e Dosagem dos Princípios Antimaláricos nos Chás do Caule e Raiz. Dissertação de Mestrado em Química, Universidade Federal do Amazonas, Manaus, AM, Brasil.
- Saraiva, R. C. G., Barreto, A.S., Siani, A.C., Ferreira, J.L.P., Araujo, R.B., Nunomura, S.M. & Pohlit, A.M. (2002). Anatomia foliar e caulinar de *Picrolemma sprucei* Hook (Simaroubaceae). *Acta Amazonica*. 33(2) 213-220.
- Shou, W. Z. (2020). Current status and future directions of high-throughput ADME screening in drug discovery. *Journal of Pharmaceutical Analysis*, 10(3), 201-208.
- Silva, E. C. C. (2006). Isolamento, transformação química e atividade biológica *in vitro* dos quassinóides neosergeolida e isobruceína B. Dissertação de mestrado. Universidade Federal do Amazonas, Manaus, Amazonas. 2006.
- Thomas, W. W. (1990) The American genera of Simaroubaceae and their distribution. *Acta Botanica Brasílica*, 4 (1), 11-18.
- Tyburn, J. M. & Coutant, J. (2016). TopSpin ERETIC 2 - Electronic to Access *In vivo* Concentration User Manual, 1-34.
- Vieira, I. J. C., Rodrigues, E., Fernandes, J. B. & Silva, M. F. G. F. (2000). Complete ¹H and ¹³C chemical shift assignments of a new C22-quassinoid isolated from *Picrolemma sprucei* Hook by NMR spectroscopy. *Magnetic Resonance in Chemistry*, 38, 805-808.
- World Health Organization. (2021). *Coronavirus disease (COVID-19) situation reports*. Retrieved from <https://www.who.int/emergencies/diseases/novel-coronavirus-2019>. Accessed 19 June 2021.
- Wu, C., Liu, Y., Yang, Y., Zhang, P., Zhong, W., Wang Y, Wang, Q., Xu, Y., Li, M., Li, X., Zheng, M., Chen, L. & Li, H. (2020) Analysis of therapeutic targets for SARS-CoV-2 and discovery of potential drugs by computational methods. *Acta Pharmaceutica Sinica B*, 10(5), 766-88.
- Wu, Y. & Wang, G., Machine Learning Based Toxicity Prediction: From Chemical Structural Description to Transcriptome Analysis. (2018). *International Journal of Molecular Sciences*, 19(8), 2358.
- Yu, R., Chen, L., Lan, R., Shen, R. & Li, P. (2020). Computational screening of antagonist against the SARS-CoV-2 (COVID-19) coronavirus by molecular docking. *International Journal of Antimicrobial Agents*, 2020; 56(2), 106012.
- Zaheer-Ul-Haq, Halim, S. A., Uddin, R., & Madura, J. D. (2010). Benchmarking docking and scoring protocol for the identification of potential acetylcholinesterase inhibitors. *Journal of Molecular Graphics & Modelling*, 28(8), p. 870-882.
- Zhu, N., Zhang, D., Wang, W., Li, X., Yang, B., Song, J., Zhao, X., Huang, B., Shi, W., Lu, R., Niu, P., Zhan, F., Ma, X., Wang, D., Xu, W., Wu, G., Gao, G. F., Tan, W., & China Novel Coronavirus Investigating and Research Team (2020). A Novel Coronavirus from Patients with Pneumonia in China, 2019. *The New England journal of medicine*, 382(8), 727-733.
- Zukerman-Schpector, J., Castellano, E. E., Fho, E.R. & Vieira, I. J. C. (1994). A new quassinoid isolated from *Picrolemma pseudocoffea*. *Acta Crystallographica C*, 50, 794-797.